AD-A168 489 NITRIC OXIDE AND NITROGEN DIOXIDE CONTENT OF WHOLE AIR SAMPLES OBTAINED A..(U) AIR FORCE GEOPHYSICS LAB HANSCOM AFB MA C C GALLAGHER ET AL. 20 AUG 85 1/1

UNCLASSIFIED F/G 4/1 NL

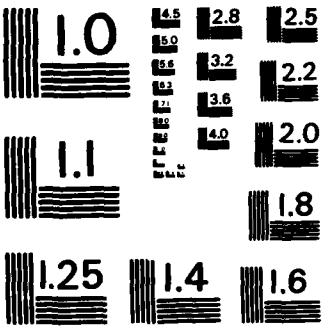

JOURNAL OF GEOPHYSICAL RESEARCH, VOL. 90, NO. D5, PAGES 7899–7912, AUGUST 20, 1985

Nitric Oxide and Nitrogen Dioxide Content of Whole Air Samples Obtained at Altitudes From 12 to 30 km

CHARLES C. GALLAGHER, CHARLES A. FORSBERG, ROBERT V. PIERI, GERARD A. FAUCHER, AND JOSEPH M. CALO

Air Force Geophysics Laboratory, Hanscom Air Force Base, Massachusetts

Whole air samples were obtained in the stratosphere using a liquid helium-cooled cryosampler mounted on a balloon platform. Approximately 1 g mol of sample was obtained at each of three altitudes per balloon flight and was maintained at 4 K until desorption just prior to analysis. Samples were obtained at six altitudes ranging from 12 to 30 km and at five latitudes from 9° to 64°N. Nitric oxide and the sum of nitric oxide and nitrogen dioxide content of the samples were determined using two chemiluminescence analyzers. Results from flights conducted between 1977 and 1981 are correlated with atmospheric motions and other significant variables and evaluated in terms of both one- and two-dimensional models of the stratosphere.

1. Introduction

Concern arose in the early 1970's that anthropogenic influences might lead to catalytic destruction of the ozone layer. Oxides of nitrogen from the exhausts of supersonic transports [*Johnston*, 1971] and photodissociation of fluorocarbons as they diffuse upward [*Molina and Rowland*, 1974] were postulated to be the principal agents. Subsequent studies have diminished the level of concern over aircraft emissions [e.g., *Oliver et al.*, 1977]. Nevertheless, sufficient uncertainty exists regarding the fate of the ozone layer [*Federal Aviation Administration*, 1981; *National Research Council*, 1983] to warrant continued investigation.

A research program was initiated at Air Force Geophysics Laboratory (AFGL) (then Air Force Cambridge Research Laboratories) to obtain whole air samples in the stratosphere using a balloon platform. The air was to be sampled cryogenically, maintained as a cryofrost near 4 K until just prior to analysis, and subsequently analyzed for NO_x and fluorocarbon content. A major advantage of this approach is that it affords the opportunity to obtain values for both NO and NO_x simultaneously, a situation not possible with most of the alternate experimental techniques reported. A series of 24 balloon flights was conducted between 1975 and 1981. NO and NO_x results from flights conducted between 1977 and 1981 are reported herein and compared with the predictions of several stratospheric models. Also, individual measurements are correlated with specific air masses, tropopause height differences, and diurnal variations. At the lower altitudes, possible hyrocarbon influences and local anthropogenic sources are also considered. The fluorocarbon results have been reported separately [*Gallagher et al.*, 1983].

2. Experimental

2.1. *Program Overview*

Whole air sampling is accomplished using an evacuated cylinder immersed in a dewar of liquid helium. Initially, a single sample was obtained (~1 g mol) per flight. Subsequently, a sampler with three sample chambers (trisampler) was incorporated into the program. The trisampler captured air samples at three altitudes on a single flight. Sampling is initiated by a remotely activated valve. The sampling rate can be maintained sufficiently low so that molecules deposit on first contact with a near 4 K surface. This technique avoids creation of a potentially dense, cooled gaseous cloud within the sample chamber. Metastable species are therefore collected without alteration of mixing ratios.

The cross section of the trisampler is shown in Figure 1. The nested chambers for liquid helium, liquid nitrogen, and vacuum provide a sample holding time of about 28 hours under static conditions. Details of the rest of the flight package and the flight profile are described elsewhere [*Gallagher et al.*, 1981, 1983]. Typically, the balloon is launched at dawn so that sampling is restricted to daylight hours. Three samples are obtained per flight and maintained near 4 K from the time of the sampling until desorption just prior to analysis.

Samples are collected only during the descent phase (typically at a rate of 30 m/min). An axial fan, downstream of the sampling valves, draws air up from below the gondola through a stainless steel intake tube, 7.6 cm in diameter and 6 m in length.

Chamber flow tests (C. Sherman, private communication, 1983) show that the volumetric displacement of the fan is relatively steady at about 40 cfm (19 L/s) for altitudes below 25 km, with a decrease in efficiency above this altitude. At 30 km, the operation is about two-thirds the rated capacity. These conditions result in a laminar flow regime at all but the lowest sampling altitudes where the flow is in the transitional flow regime. At the sampling point, air is drawn into one of three 2.5-cm OD tubes (one for each cryosampler volume), located radially 120° apart such that they terminate at the circumference of a 2.5-cm circle concentric with the tube. Thus the sample is effectively drawn from the central 2.5-cm-diameter core of the flow in the sampling tube. The potential effects of this flow field and passage through the sampling tube are addressed in the next section.

The intake tubing undergoes a thorough cleaning prior to launch day and is then encased in polyethylene which is pulled away at launch. A trickle flow of helium is maintained through the tubing from the encasement until shortly prior to launch [*Gallagher et al.*, 1981, 1983].

2.2. *Sampling Tube Characteristics*

Once the air sample is removed from the ambient stratosphere, the photolytic mechanisms driving the in situ, steady

Paper number 5D0141.

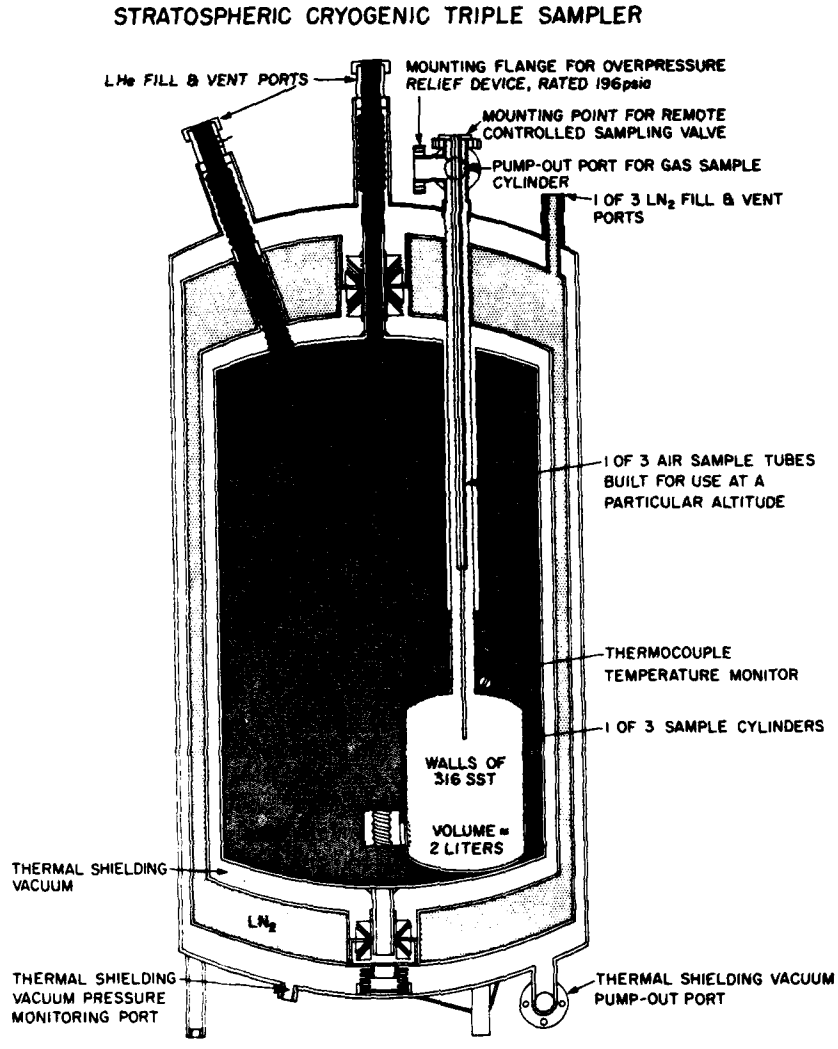

Fig. 1. Cryogenic, triple sampler used to obtain whole air samples at three stratospheric altitudes per balloon flight. Overall height is 127 cm, liquid nitrogen capacity is 24 L, and liquid helium capacity is 42 L. The internal air sample tubes are designed for specific altitudes so that a 1 g mol sample quantity can be obtained in about 50 min.

state chemistry cease. Thus the composition of the sample can relax during its passage to the sampler. Radial diffusion to the tube walls may play a role in altering the composition from that in the ambient as a result of selective loss/production of certain species and/or heterogeneous reactions. Thus it is important to consider these issues in the sampling context. In this regard, it is quite difficult to precisely duplicate in the laboratory all the conditions that characterize the operation of the sampling tube in the stratosphere. For the current work, a numerical model was developed to assess species behavior in the sampling tube. The results of a recent study using this model [*Calo*, 1984] are summarized herein.

The model is based on the application of a general purpose, homogeneous, multireaction chemical kinetics code (CHEMSEN) [see *Kramer et al.*, 1982] to a 32 reaction (50 when heterogeneous wall loss is included), 23 species (42 with adsorbed or heterogeneously consumed species) stratospheric kinetic model (see Table 1), modified to take into account heterogeneous interactions with the tube wall. The rate parameters were taken primarily from a *National Aeronautics and Space Administration* [1982] report, and representative ambient concentrations were obtained from a *World Meteorological Organization* [1982] report and from *Fabian et al.* [1982].

Since the basic code as originally developed was intended for homogeneous batch reaction systems (i.e., "closed" homogeneous chemical kinetic systems), heterogeneous wall loss rates due to radial diffusion had to be estimated and transformed into equivalent pseudohomogeneous reactions. This approach exploited the difference in time scales for radial diffusion (τ_d) and axial convection (τ_c) in the sampling tube. For $\tau_d \ll \tau_c$ (as is the case for altitudes above ~ 20 km), the steady state radial concentration profile due to diffusion is rapidly established in comparison to the residence time in the sampling tube, assuming the familiar Bessel function form for cylindrical geometry. This profile was used to obtain an analytical expression for the effective pseudohomogeneous, first-order rate constant k' for the wall loss as a function of the fraction f of the upper limit rate for instantaneous reaction at the wall (i.e., the completely diffusion-limited case, $f = 1$). In other words, the heterogeneous wall loss rate was transformed to

$$-r_{wall} = k'C_m$$

where C_m is the mean concentration of a particular species in

TABLE 1. Stratospheric Kinetic Model

Number	Reaction	k_2 A_0,* (s mol/cm³)⁻¹	k_2 E,* cal/mol
	Bimolecular Reactions		
1.	$O + O_3 \rightarrow 2O_2$	0.90×10^{13}	4407.
2.	$NO_2 + O \rightarrow NO + O_2$	0.56×10^{13}	0.
3.	$O_3 + NO \rightarrow NO_2 + O_2$	0.13×10^{13}	2841.
4.	$NO + ClO \rightarrow NO_2 + Cl$	0.37×10^{13}	−584.
5.	$NO + HO_2 \rightarrow NO_2 + HO$	0.22×10^{13}	−477.
6.	$NO_2 + O_3 \rightarrow NO_3 + O_2$	0.72×10^{11}	4868.
7.	$NO_3 + NO \rightarrow 2\,NO_2$	0.12×10^{14}	0.
8.	$HNO_4 + HO \rightarrow NO_2 + H_2O + O_2$	0.78×10^{12}	−755.
9.	$HNO_3 + HO \rightarrow NO_3 + H_2O$	0.57×10^{10}	−1546.
10.	$HO_2 + HO \rightarrow H_2O + O_2$	0.48×10^{14}	0.
11.	$HO_2 + HO_2 \rightarrow H_2O_2 + O_2$	0.18×10^{13}	0.
12.	$HO_2 + O \rightarrow HO + O_2$	0.18×10^{14}	−397.
13.	$HO_2 + ClO \rightarrow HOCl + O_2$	0.28×10^{12}	−1411.
14.	$HO_2 + O_3 \rightarrow HO + 2O_2$	0.84×10^{10}	1152.
15.	$HO + O_3 \rightarrow HO_2 + O_2$	0.96×10^{12}	1868.
16.	$HO + O \rightarrow H + O_2$	0.132×10^{14}	−232.
17.	$HO + CO \rightarrow H + CO_2$	0.81×10^{11}	0.
18.	$HO + H_2 \rightarrow H + H_2O$	0.37×10^{13}	4034.
19.	$H_2O_2 + HO \rightarrow H_2O + HO_2$	0.19×10^{13}	372.
20.	$Cl + O_3 \rightarrow ClO + O_2$	0.17×10^{14}	511.
21.	$ClO + O \rightarrow Cl + O_2$	0.46×10^{14}	258.
22.	$N_2O_5 + M \rightarrow NO_2 + NO_3 + M$	0.14×10^{00}	0.
23.	$Cl + H_2 \rightarrow H + HCl$	0.22×10^{14}	4570.
24.	$HO_2 + Cl \rightarrow O_2 + HCl$	0.11×10^{14}	−338.
25.	$HO_2 + Cl \rightarrow OH + ClO$	0.25×10^{14}	894.

Number	Reaction	k_3 A_0,† [s (mol/cm³)²]⁻¹	β
	Termolecular Reactions		
26.	$O + O_2 + M \rightarrow O_3 + M$	0.20×10^{20}	− 2.3
27.	$NO_2 + O + M \rightarrow NO_3 + M$	0.39×10^{21}	− 2.0
28.	$NO_2 + HO + M \rightarrow HNO_3 + M$	0.53×10^{25}	2.9
29.	$NO_2 + HO_2 + M \rightarrow HNO_4 + M$	0.21×10^{29}	− 4.6
30.	$NO_3 + NO_2 + M \rightarrow N_2O_5 + M$	0.69×10^{25}	− 2.8
31.	$H + O_2 + M \rightarrow HO_2 + M$	0.59×10^{20}	− 1.4
32.	$ClO + NO_2 + M \rightarrow ClONO_2 + M$	0.173×10^{26}	− 3.4
	Heterogeneous Reactions		
33.	$NO \rightarrow NO$ (*)		
34.	$NO_2 \rightarrow NO_2$ (*)		
35.	$N_2O_5 \rightarrow N_2O_5$ (*)		
36.	$NO_3 \rightarrow NO_3$ (*)		
37.	$HNO_3 \rightarrow HNO_3$ (*)		
38.	$HNO_4 \rightarrow HNO_4$ (*)		
39.	$O \rightarrow O$ (*)		
40.	$O_3 \rightarrow O_3$ (*)		
41.	$HO \rightarrow HO$ (*)		
42.	$HO_2 \rightarrow HO_2$ (*)		
43.	$H_2O_2 \rightarrow H_2O_2$ (*)		
44.	$Cl \rightarrow Cl$ (*)		
45.	$ClO \rightarrow ClO$ (*)		
46.	$H \rightarrow H$ (*)		
47.	$HOCl \rightarrow HOCl$ (*)		
48.	$H_2O \rightarrow H_2O$ (*)		
49.	$ClONO_2 \rightarrow ClONO_2$ (*)		
50.	$HCl \rightarrow HCl$ (*)		

From *National Aeronautics and Space Administration* [1982, Tables 1 and 2].

*$k_2 = A_0 \exp(-E/RT)$, (s mol/cm³)⁻¹ (Table 1).

†$k_3 = A_0\, T^{\beta}$, [s (mol/cm³)²]⁻¹ (Table 2).

the sampled central core of the flow in the sampling tube, obtained from the Bessel function profile. In this expression, for $f = 0$, $k' = 0$; for $f = 1$, $k' = (2.4)^2 D/R^2$ (where D is the diffusivity of the species and R is the tube radius), which is the inverse of the characteristic time for diffusion to the tube walls, and for $0 < f < 1$, $k' = \alpha_1$, where α_1 is given by the solution of the transcendental equation, $\phi = 1.45f/J_1(0)$, and $\phi = (\alpha_1/D)^{1/2}R$. For further details of the model and method of solution see *Calo* [1984].

For all the species of direct interest here, it was found that the gas phase chemistry was incapable of appreciably altering the sampled composition from that in the ambient. This was due to the fact that the average residence time in the sampled central core (e.g., 1.4 s at 20 km) was significantly less than the time constants of most of the stratospheric reactions in the model. Consequently, the most dramatic change in composition is the rapid decrease in O atom concentration due to termolecular reaction with O_2. The half-life of O in the sampling tube due to this reaction varies from 1.7×10^{-4} s at 15 km, to 0.024 s at 30 km. Two other species sensitive to flow in the sampling tube are Cl and NO_3. They are capable of exhibiting significant increases in concentration due to homogeneous gas phase reactions during passage. The magnitude of this enhancement is sensitive to heterogeneous wall loss at higher altitudes. In any case, the observed alterations in sampled ambient composition due to homogeneous gas phase reactions, had no effect on the major species, including NO_x.

Therefore the model results are conclusive in showing that the only manner in which the sampling tube can appreciably alter the sampled composition from that in the ambient is via heterogeneous interactions with the tube wall. Currently, definitive assessments of the impact of heterogeneous processes at the tube wall on gas phase composition are hampered by lack of knowledge concerning the controlling phenomena at stratospheric conditions. Therefore the potential effects of the tube wall were examined parametrically with the model with respect to the previously defined fraction f of the upper limit instantaneous wall destruction rate.

Examples of results from some of these studies are presented in Table 2 for a few cases at three altitudes. Two different sets of ambient values for NO and NO_2 mixing ratios were examined, an average of the mid-latitude measurements reported herein and those estimated by *Fabian et al.* [1982]. A comparison of the NO/NO_2 ratio for cases 1 and 3 ($f = 0$) with their respective ambient values (i.e., the ratios determined with respect to the ambient mixing ratios assumed at the sampling tube mouth), clearly shows that homogeneous gas phase chemistry in the sampling tube is incapable of appreciably altering the NO_x content of the stratospheric air samples, as was indicated above.

The effects of any heterogeneous interactions would be most severe at the highest altitudes where radial diffusivities are greatest. At the expected tube wall temperatures at 30 km (i.e., 230–260 K), capture (i.e., condensation) coefficients close to unity (i.e., $f = 1$) are highly improbable for most of the major species considered here. For example, consider NO_2 which is more condensable than NO. At 30 km, for a mixing ratio of 10.8 ppbv, the average of the mid-latitude values reported herein, the incident wall flux of NO_2 is approximately 3×10^{10} molecules/cm² s. In the absence of significant heterogeneous reactions on the tube wall, the capture coefficient of a species is determined by the net difference between the incident and evaporative wall fluxes. The corresponding evaporative fluxes of NO_2, estimated from vapor pressures (actually of N_2O_4) at 230 and 260 K are about 2×10^{21} and 4×10^{22} molecules/cm² s, respectively. Under these conditions, NO_2 cannot be absorbed onto the wall to any appreciable extent, and thus its capture coefficient should be small. On the other hand, loss coefficients close to unity due to heterogeneou

TABLE 2. Ratios of Selected Species Concentrations for Four Computational Cases

	Ambient	Case 1	Case 2
	15 km		
NO/NO_2	0.714	0.706	0.708
$NO/[NO + NO_2]$	0.417	0.414	0.414
$NO/[NO + NO_2 + HNO_3]$	0.306	0.303	0.304
	Ambient	Case 3	Case 4
NO/NO_2	1.00	0.980	0.985
$NO/[NO + NO_2]$	0.50	0.495	0.496
$NO/[NO + NO_2 + HNO_3]$	0.029	0.029	0.029
	Ambient	Case 1	Case 2
	20 km		
NO/NO_2	0.558	0.547	0.550
$NO/[NO + NO_2]$	0.358	0.353	0.355
$NO/[NO + NO_2 + HNO_3]$	0.189	0.186	0.187
	Ambient	Case 3	Case 4
NO/NO_2	0.333	0.327	0.329
$NO/[NO + NO_2]$	0.250	0.247	0.248
$NO/[NO + NO_2 + HNO_3]$	0.016	0.015	0.155
	Ambient	Case 1	Case 2
	30 km		
NO/NO_2	0.528	0.549	0.551
$NO/[NO + NO_2]$	0.345	0.354	0.355
$NO/[NO + NO_2 + HNO_3]$	0.253	0.187	0.187
	Ambient	Case 3	Case 4
NO/NO_2	0.20	0.196	0.199
$NO/[NO + NO_2]$	0.167	0.164	0.166
$NO/[NO + NO_2 + HNO_3]$	0.083	0.082	0.083

Ambient: ratios for assumed ambient composition with NO and NO_2 mixing ratios taken as the average of all mid-latitude data reported herein. Case 1: ratios at the sampling point for the assumed ambient composition at the tube inlet with $f = 0$ for all species, i.e., homogeneous gas phase chemistry only. Case 2: ratios at the sampling point for the assumed ambient composition at the tube inlet with $f = 1$ (i.e., instantaneous wall loss) for all species except NO, NO_2, HNO_3, CO, CO_2, O_2, N_2, and H_2, for which $f = 0$. Cases 3 and 4 are equivalent to cases 1 and 2, respectively, except that the NO and NO_2 mixing ratios assumed for the ambient composition are taken from *Fabian et al.* [1982].

reaction at the wall are quite probable for most of the reactive radical species considered in the current model. However, heterogeneous reactions of both NO and NO_2 at the tube wall, leading to interconversion of the acids of the oxides of nitrogen, are rather unlikely. Under the ambient operating conditions of the sampling tube, the tube wall should be relatively free of even the water vapor condensate required to form the acids. Assuming a water vapor mixing ratio of ~3 ppmv at 30 km, the maximum wall flux is approximately 8×10^{12} molecules/cm^2 s, in comparison to an evaporative flux of about 40×10^{19} and 8×10^{20} molecules/cm^2 s, at 230 and 260 K, respectively. Thus in summary, it is quite unlikely that heterogeneous interactions with the sampling tube wall will alter the ambient composition of the sample with respect to NO and NO_2.

In Table 2, cases 2 and 4 give the model results for the most likely conditions in the sampling tube consistent with the preceding. The ratios determined for those two cases are actually closer to the ambient values than those for cases 1 and 3. This behavior is due to the fact that some radical species responsible for destruction of NO_x species are assumed to be completely lost at the sampling tube walls for cases 2 and 4.

Other factors might make the sampling tube more effective in altering the ambient composition. One such possibility is solar heating of the sampling tube, which if significant, would increase rate constant values over those assumed. Available data from the flight data included air temperature and surface temperature on the main gondola package (which should be similar to that of the sampling tube surface). These data indicate a maximum surface temperature deviation of about 9°C. More recently, the same sampling tube was used in another air sampling program in the lower stratosphere, and thermistors were attached to the tubing at various locations. The maximum surface temperature throughout the 18- to 13-km sampling range was −17°C. Consideration of the steady state energy balance on the sampled air clearly indicated that temperature differences far in excess of those measured for extended periods of time, would be required in order to cause any significant temperature change in the sampled air during its passage through the sampling tube. In this manner, temperature effects were easily dismissed as a significant factor [cf. *Calo*, 1984].

Various configurations of stainless steel and Teflon tubing were employed to transmit test samples to the input of each chemi-analyzer, and as inlet tubing for the "dry run" sampling system. Results indicated that alteration of the test samples was well within the quoted experimental uncertainties. This point is discussed further in the following two subsections. Therefore use of the stainless steel intake tube was deemed acceptable for the balloon flights.

2.3. *Sample Storage Characteristics*

For reactive species such as NO and NO_2, careful consideration must also be given to possible alteration of their relative ambient concentrations during residence in the cryofrost, during the subsequent desorption process, as well as during the comparatively brief time between desorption and analysis. Studies of the behavior of these species within a cryofrost and during desorption have been carried out at higher cryofrost temperatures and much higher reactive species mixing ratios than encounterd in the present investigation. *Addison and Barrer* [1955] reported significant disproportionation of pure NO to NO_2, N_2O, N_2O_3, and N_2 upon desorption from cold zeolites and charcoal adsorbents. *Fezza and Calo* [1982] and *Calo et al.* [1981] also reported the disporportionation of pure NO collected as a cryofrost on a 15 K gold-flashed, stainless steel surface upon subsequent thermal desorption. Approximately two-thirds of the NO originally deposited was converted to NO_2, consistent with the stoichiometry: $4NO \rightarrow N_2 \rightarrow 2NO_2$. However, these reactions are related to the association of NO in the cryofrost, which has been shown by infrared spectrophotometry to be almost entirely dimerized for pure NO under these conditions [*Smith et al.*, 1951]. This situation is in direct contrast to the present work, where NO is totally isolated due to its extreme dilution in the air matrix. Thus the net effect of similar alterations in our samples was expected to be negligible. Indeed, laboratory cryogenic sampling "dry runs" with NO, NO_2, and H_2O at typical stratospheric concentrations in air, including storage and subsequent thermal regeneration in exactly the same manner as for actual air samples, revealed only negligible alteration of the original sample; i.e., variations in measured NO and NO_2 were well

within the uncertainty limits reported here for the stratospheric measurements.

Fezza and Calo [1982] and *Calo et al.* [1981] also observed some oxidation of NO to NO_2 [~19%] by ozone over and above that expected due to pure NO disproportionation for cryofrost matrices composed of 1/1/44.4 for $NO/O_3/O_2$ upon desorption from a gold-flashed stainless steel surface maintained at 15 K during deposition. However, 2.25% ozone in an oxygen matrix was found to recombine almost completely upon thermal desorption for total ozone deposits of less than about 5×10^6 g mol [*Calo et al.*, 1981]. Thus small amounts of ozone, less than a threshold level, were found to recombine completely upon thermal desorption from the solid. In the context of the present work, any ozone originally collected would not survive cryofrost regeneration, nor could it oxidize appreciably the very small amount of NO present. A related consequence is that no ozone is available to oxidize NO in the gas phase after warmup. Finally, the rate of oxidation of NO by ozone and/or oxygen in the solid cryofrost has been found to be much too slow to cause any alteration of the original NO/NO_2 concentrations [*Lucas and Pimental*, 1979; *Smith and Guillory*, 1977].

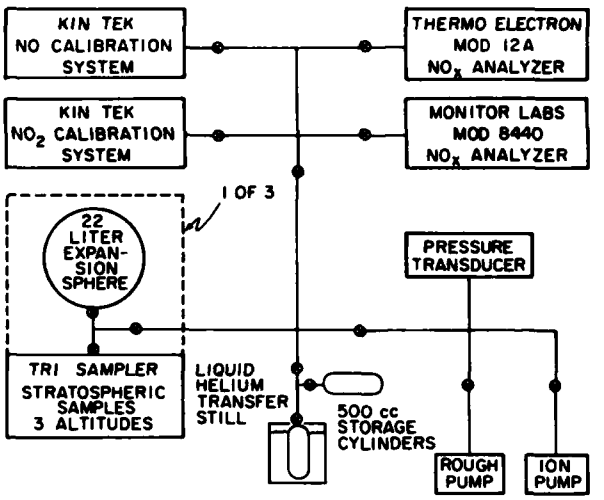

Fig. 2. Manifold that permits simultaneous desorption of all three samples into individual spheres, after which, sequentially, each sample is analyzed for NO and NO_x content, with the balance of the sample then transferred cryogenically into storage cylinders.

2.4. *Sample Manipulation and Analysis*

The samples are returned to the laboratory for desorption followed by analysis using chemiluminescence analyzers. The trisampler is connected to the manifold as illustrated in Figure 2. The pump-out valve on each sample chamber is connected to a stainless steel sphere and to the manifold. Each sphere was passivated with either gold or hexamethyldisilazane (HMDS) and then evacuated on a separate vacuum system before connection to the manifold. Both surface treatments are acceptable for the present application with respect to lack of chemical reactivity. Apparently, HMDS was first used for this purpose by *Schmeltekopf et al.* [1976]. HMDS is better than gold for accommodating and stabilizing condensation at cryofrost surfaces due to its relatively higher number of effective surface condensation sites [*Calo et al.*, 1981]. Tests conducted using both gold and HMDS-coated spheres yielded results that were within 5% of one another, which can easily be accounted for by slight differences in the passivation process history for each sphere and variance in the chemiluminescence measurements. Only gold seal valves and gold-plated copper gaskets are used in the stainless steel manifold. Generally, the small portion of the manifold that comes in contact with the sample at this time is also gold plated.

After evacuation of the manifold, each sphere/valve combination is isolated from the manifold by valve closures and then opened to each other. The trisampler guard vacuum is then released, resulting in a rapid cryogen boil-off. Following cryogen depletion, a flow of slightly warmed air is directed into the liquid helium chamber to accelerate sample warmup. The temperature-time history of the warmup is approximately exponential, achieving room temperature within about 18 hours. At this point, high boiling point species, such as NO_2, have been quantitatively returned to the gaseous state, and thus analysis can then begin. Each sample attains an absolute pressure of about 700 mm Hg. The pressure of the first sample is measured, and then portions of it are introduced sequentially into the chemiluminescence analyzers with each flow maintained for several minutes. The remainder of the sample then becomes available for analysis by gas chromatography to determine the stable species content. The manifold is then reevacuated, and analyses of the second and third samples are performed in a similar manner. The NO_x analyses are completed within 1–6 hours of commencement, depending on the number of samples to be analyzed.

Two chemiluminescence analyzers were used, a Thermo Electron Corp. model 12A plus a Monitor Labs model 8440B (incorporated after 1977). Both were modified "in house" to optimize measurements of low NO_x concentrations. A more sensitive amplifier was installed in the model 12A and zero balance achieved with a Keithley model 261 picoampere source. The output is displayed on a Keithley model 640 electrometer and is recorded as well. External pumping is employed for the model 8440B, and special internal orifices were installed for optimum detection of low mixing ratios.

With these modifications to each instrument the detection limits were determined to be 0.1 ppbv for the TE 12A and 0.25 ppbv for the ML 8440B. For each sample, the signals, integrated over the duration of the analysis, are reported as the measured values. Long-term integration is particularly important near the detection limit. This approach raises the question of whether or not there is any drift with time in the mixing ratios of NO or NO_x. As a check on the stability of the concentrations of these species over the measurement period, chemiluminescence analyzer output was studied as a function of time. Typically, each sample was analyzed continuously for several minutes to take advantage of the large quantities of sample, thereby yielding more data and reducing measurement error. We concluded that after steady state is attained, generally within the first few seconds of flow, no discernible drift in species mixing ratios occurs over the duration of the measurement. Each data set was carefully evaluated for the attainment of steady state conditions. Hence on occasion, the first 2 min of data, for example, were eliminted from a 15-min analysis period. A constant input flow to the instruments was maintained during sampling by adjustment of a needle valve at the input of the TE 12A and by an internal regulator for the ML 8440B.

In addition to the usual gain in measurement precision afforded by use of two instruments, a precaution against detection of another chemiluminescent reaction was also achieved, since each instrument employs a different filter/photomultiplier sensitivity combination. In the instruments, the excited

species NO_2* reverts to lower energy states, emitting broadband radiation extending from 5000 to 30,000 Å with maximum intensity at about 11,000–12,000 Å. The TE 12A contains a photomultipler tube which has a peak sensitivity at 7500 Å. The filter is a Corning P-64, which has 1% transmission at 6500 Å and 0% at 6000 Å. The ML 8440B unit photomultiplier tube has peak sensitivity near the low end of the broad emission band but is sensitive into the near infrared, and it too has a filter that eliminates the blue region where other likely chemiluminescent reactions may contribute, such as for some unsaturated hydrocarbons. Thus with each unit having a characteristic response over a different limited bandwidth, there is a reduced possibility for other chemiluminescent reactions contributing to the quoted NO_x values. Alternately, if there was an interfering reaction, it would produce a consistently enhanced signal on one of the units, an event not observed. Some other differences between the two instruments include the use of two channels on the ML 8440B to provide simultaneous readout of both NO and NO_2, the use of a stainless steel converter and primarily polyethylene tubing in the TE 12A, and a molybdenum converter in the ML 8440B along with predominantly Teflon tubing. The stainless steel converter operates at a higher temperature, thereby increasing the possibilities for detection of additional compounds. However, as indicated, a consistently enhanced signal was never observed on either instrument; i.e., any differences in output were always with the expected variance of the measurements.

Originally, all instrument calibrations were performed by means of a dynamic dilution of separate purchased standards of NO and NO_2 in N_2 or He, utilizing a Thermo Electron Corp. Series 101 dynamic NO-NO_2-O_2 calibrator supplied with smaller than standard control orifices. Ultrahigh purity nitrogen (99.999%) was used as the mixing gas, and the purchased standards were generally supplied in aluminum cylinders with an aluminum oxide surface enhanced by an anodizing process that eliminates pinhole porosity. An additional proprietary step has been taken to improve further the stability of the gas mixture (AIRCO Corp., Spectra Seal Cylinders).

Periodically, a flow of the ultrahigh purity nitrogen was directed into the analyzers to determine the NO_x content of the mixing gas. A second calibration method, phased into the system in 1978, became the sole method in 1980. The latter is based on the permeation of the test gas through a Teflon membrane into a flow of ultrahigh purity nitrogen. Separate units were incorporated for NO and NO_2 (Kin Tek Corp. models 570 and 670). Calibration plots were obtained for the NO_x analyzers by varying permeation tube temperature and nitrogen flow rate. A portion of the mixture was vented through a flowmeter in order to maintain the required pressure drop. The response for both analyzer systems was found to be linear, and the measured NO_2 volume mixing ratios exhibited agreement with the calibration inputs to within 5%. Permeation rates for the Kin Tek Corp. tubes are certified by the manufacturer. These permeation rates represent weight losses of only 0.1 mg over several hours from a tube that weights several hundred grams. Subsequent to the 1981 flights, a high-capacity precision balance was obtained that permitted accurate measurements of the weight losses from sealed tubes (such as the NO_2 tube) used for this and other experiments [*Gallagher and Forsberg*, 1983]. Although the Kin Tek NO_2 tube used for our investigations developed a leak (presumably around the Teflon seal) subsequent to the 1981 measurements, weight loss measurements performed with other Kin Tek tubes using this new analytical balance (Mettler Corp. model H315 Macro Analytical, High Capacity Balance; weighing range 1001 g, readability 0.1 mg, precision ±0.1 mg) indicated permeation rates that remained within a few percent of the factory calibration values. NO_2 calibrations have the added value of testing both the efficiency of the converter and the accuracy of the reaction chamber. The analyzer response for low mixing ratios of NO_2 was further checked at a later date using a second permeation system (Vici Metronics model 415) which features a much lighter weight sealed tube (approximately 18 g); the measured mixing ratios were within 5% of predicted values. Permeation rates based on laboratory weight loss determinations agreed with the factory-determined permeation rates to within 10%. Both Teflon and stainless steel tubing of vairous test lengths were utilized (exclusive of the transfer manifold) for both calibration and test sample runs. No sample alterations due to tubing material/length variations could be discerned under steady state operating conditions.

Nitric oxide calibrations were also performed. The reaction chamber of the TE 12A had already been tested with the NO_2 calibrations, but since the ML 8440B employs separate chambers for the NO_2 and NO measurements, it was decided to obtain independent NO calibrations. The Kin Tek NO tube was recharged within the model 570 unit for each calibration series, and thus mixing ratio determinations were based solely on the factory-supplied permeation rates. Since both analyzer responses agreed to within 10% of the calibration gas mixing ratios, the reliability of the NO reaction chambers of both instruments was confirmed. (The TE 12A reaction chamber reliability was also checked by the more extensive NO_2 tests.) All NO permeation tube calibrations were performed frequently with the Kin Tek system, since Vici Corp. did not offer an NO tube. Two methods were used to balance the chemiluminescence analyzers for zero NO and NO_2 input. Initially, the input valve of the TE 12A would be closed and the zero adjusted. Later (with both instruments), grade 6 helium (99.9999% purity) was introduced at the sample gas inlet during the zeroing procedure. These methods were determined to be superior to the use of ultrahigh purity nitrogen, which could still contain nonnegligible concentrations of the species to be measured, although the calibration plots obtained subsequently showed the NO contribution to be essentially zero and the NO_2contribution slight but also negligible.

Both analyzers were tested for their response to HNO_3. The Vici Metronics Dynacalibrator was utilized with an HNO_3 permeation tube. A mixing ratio of 11.3 ppbv was produced, a value representative of the highest mixing ratio that might be expected for the altitude range of interest. Both the NO and NO_x responses of the two analyzers were monitored and found to be essentially zero in all cases. Weight loss was also determined for the HNO_3 tube using the Mettler balance. The results agreed with the predicted weight loss based on the factory-certified permeation rate.

Other stratospheric species suspected of potentially affecting the NO_x measurements were N_2O_5 and NO_3. *Fabian et al.* [1982] reported mid-latitude model values for N_2O_5 that increased from 0.6 pptv at 12 km to 0.3 ppbv at 30 km. Thus even if N_2O_5 could contribute to the measured signals, it would have a negligible effect on the quoted values of NO_x below 25 km, increasing to a maximum of 1 5% at 30 km. *Fabian et al.* [1982] also gave model values for NO_3 ranging from 0.0001 pptv at 12 km to 0.3 pptv at 30 km. Thus again, even if detectable, NO_3 would provide a negligible contri-

TABLE 3. Flight Data Plus NO and NO_x Results

Flight No.	Date	Site	Lat.	Alt., km	T.A.S., hours	Tropopause Height, km	NO, PPBV	NO_x, PPBV
11*	Oct. 8, 1977	Chico, CA	40N	30	3.7	11.8	1.0 ± 0.4	1.7 ± 0.7
12*	Oct. 17, 1977	Chico, CA	40N	18	4.1	10.4	1.3 ± 0.5	4.3 ± 1.7
13*	June 2, 1978	Eielson AFB, AK	64N	30	5.9	8.5	8.6 ± 3.4	35.0 ± 14
				25	6.7		2.2 ± 0.9	15.2 ± 6.1
				20	9.3		1.8 ± 0.7	5.7 ± 2.3
14*	June 7, 1978	Eielson AFB, AK	64N	15	6.0	9.1	2.1 ± 0.8	2.9 ± 1.2
				12	7.2		2.1 ± 0.8	6.1 ± 2.4
15	Aug. 19, 1978	Watertown, SD	45N	15	3.8	16.1	2.3 ± 0.7	4.0 ± 1.2
				12	6.1		4.0 ± 1.2	6.8 ± 2.0
16	Aug. 29, 1978	Watertown, SD	45N	30	3.6	12.1	12.0 ± 3.6	35.0 ± 10
				25	5.6		3.6 ± 1.1	7.7 ± 2.3
				20	7.6		3.2 ± 1.0	12.3 ± 3.7
17	March 15, 1979	Panama, CZ	9N	18	3.4	17.3	1.9 ± 0.6	4.4 ± 1.3
				15	5.2		2.0 ± 0.6	5.8 ± 1.7
18	March 20, 1979	Panama, CZ	9N	30	2.9	17.6	12.7 ± 3.8	19.8 ± 6
				25	4.9		3.2 ± 1.0	5.9 ± 1.8
				20	7.8		5.9 ± 1.8	10.7 ± 3.2
19*	June 21, 1979	Holloman AFB, NM	33N	30	3.1	15.8	2.7 ± 1.1	3.2 ± 1.3
				25	5.2		1.8 ± 0.7	2.4 ± 1.4
				20	7.1		2.0 ± 0.8	2.9 ± 1.2
21	April 28, 1980	Holloman AFB, NM	33N	18	3.2	13.4	0.6 ± 0.3	2.7 ± 0.8
				15	4.3		0.5 ± 0.3	2.9 ± 0.9
				12	6.6		0.5 ± 0.3	2.0 ± 0.6
22	May 1, 1980	Holloman AFB, NM	33N	30	3.5	9.6	1.8 ± 0.5	18.7 ± 6
				25	5.7		0.4 ± 0.2	3.3 ± 1.0
				20	7.2		0.7 ± 0.3	4.0 ± 1.2
23	May 31, 1981	Holloman AFB, NM	33N	20	4.5	11.7	2.0 ± 0.6	8.7 ± 2.6
				15	6.5		0.8 ± 0.3	2.7 ± 0.8
				12	8.1		0.4 ± 0.2	1.8 ± 0.5
24	June 4, 1981	Holloman AFB, NM	33N	30	5.4	11.4	1.1 ± 0.3	2.3 ± 0.7
				25	7.4		1.3 ± 0.4	2.8 ± 0.8
				20	9.4		1.1 ± 0.3	2.6 ± 0.8

T.A.S., time after sunrise at altitude. Flight numbers 1–10, preliminary data only. No data points for small cryogenic and grab samples.
*Thermo Electron model 12A only.

bution to the signals at all altitudes studied. In summary, consideration of all of the species most likely to interfere with the measurements leads to the conclusion that even under the worst conditions their total contribution to the overall uncertainty in the quoted values is negligibly small.

Simulation runs were performed using a trisampler prepared exactly as for flight. Test samples were gathered as cryofrosts, maintained near 4 K, and then regenerated and allowed to expand into the same transfer manifold used for the flight samples. The subsequent sample introduction techniques to the chemiluminescence analyzers were also performed exactly as with the flight samples. Also, portions of the test samples were transmitted directly from the source cylinder to the analyzers. These procedures provided a test for possible alteration of sample mixing ratios in the sampling, storage, and regeneration procedures.

Results from the simulation runs for both NO and NO_x indicated that the direct measurements of the test samples were just as likely to be higher as lower than for portions of the test samples that were subjected to the entire cryocondensation, regeneration procedure in the trisampler. This indicates that random measurement errors significantly exceeded any systematic errors introduced by the cryosampling, storage, regeneration, and gas sample manipulation procedures. Our measurement errors are believed to be primarily due to unavoidable drifts in the analyzer calibrations (including both full-scale sensitivity and instrument zero), in spite of frequent checks on same. Other lesser contributions to measurement error are slight variabilities in the mixing ratios of the reference test gas.

In summary, although it was not possible to reproduce test gas samples that were exactly representative of expected stratospheric compositions (both with respect to mixing ratios and species, especially radicals), the combined results of the laboratory tests, procedures, and analysis described above, strongly support our conclusion that the sampling, storage, and regeneration procedures quantitatively preserved the species for which we report ambient mixing ratios to within the quoted tolerances. Our best estimates of these uncertainties are as follows: for NO, total uncertainty for the stratospheric sample measurments is ±30% for readings greater than 1 ppbv, increasing to ±50% below 0.5 ppbv. For NO_x, the overall uncertainty is also ±30%. For those determinations based solely on the TE 12A, the overall uncertainty is ±40 for both NO and NO_x.

3. Results and Discussion

Table 3 summarizes the more salient parameters for the balloon flights and includes the NO and NO_x (i.e., NO + NO_2) results that are the averages from the two chemiluminescence analyzers, except as indicated. Values for both species are considered reliable to within the tolerances stated above.

The balloon flights commenced in 1975, but the early flights were conducted primarily to obtain measurements of various

stable species using gas chromatography [*Gallagher et al.*, 1983], and thus only rough values for NO_x mixing ratios were obtained. The Monitor Labs unit was under repair in July 1979. On flight 20, only ambient temperature grab samples were obtained. The low sample amounts retrieved were sufficient for gas chromatographic analyses only.

The greatest spread in data, not unexpectedly, occurs for the 30 km NO_x results. The rate of change of mixing ratio with altitude has been predicted by model studies to be greater at 30 km than at any other of the altitudes investigated. Coupling this with the vertical shift in the predicted profiles required with shifts in tropopause height, the 30-km measurement altitude actually represents a significantly different position on the profile from flight to flight.

Before comparing the data from Table 3 with various model profiles or with representative results of other workers, we address the problem of why a few of the measured values seem to be at variance with the smooth profiles predicted by practically every model. The analysis that follows considers all of the data points from Table 3, but especially those that produce anomalies in the individual profiles from each test series. Of course, smooth profiles in and of themselves do not guarantee the quality of the data, but deviations from a smooth profile require more intensive evaluation.

Although various influences will be considered, the primary emphasis centers on associating the anomalies with the sampling at successive altitudes and especially different dates of portions of air that are associated with different air masses. *Noxon et al.* [1983] have discussed the effects of large-scale transport relative to NO_2 abundance. In addition, *Horvath et al.* [1983] noted significant variations in NO in the upper stratosphere and attributed them to transport processes that carry air from regions of significantly different odd-nitrogen abundances into the mid-latitude upper statosphere. *Mount et al.* [1984] obtained values for NO_2 based on the visible light spectrometer on board the Solar Mesospheric Explorer spacecraft providing daytime values for the 20- to 40-km altitude region. Their data indicate that NO_2 exhibits a strong memory of the physical conditions of the stratosphere over a period of several days. We make no effort to interpret our data variations in terms of the specifics of these detailed analyses, primarily because we do not have a sufficiently large data base covering a sufficient range of altitudes, latitudes, and seasons to provide such evaluations. We cite these references simply to point out that significant variations in NO and NO_2 mixing ratios do occur because of atmospheric motions.

Second, the association of peroxyacetyl nitrate (PAN) with the oxides of nitrogen and variability thereof in the vicinity of the tropopause will also be evaluated, and finally, the possibilities of effects from local injections are considered. Of course, the smaller ripples in the measured profiles lie well within the error bars for the data points and need not be associated with any atmospheric anomalies.

First, in order to assess whether successive samplings were actually taken from different air masses, upper air charts, appropriate to the dates and the altitudes sampled, were obtained for 200, 100, 50, 30, and 10 mbar, equivalent to 11.8, 16.2, 20.6, 23.8, and 31.0 km geopotential altitudes, respectively. Wind data from the observation station(s) closest to the sampling location provided the primary information used, although the charts were evaluated over a wide geographic region to determine the dominant wind and pressure patterns, and to be certain that the station under consideration was not reporting conditions inconsistent with the overall patterns. Table 4 indicates which charts were utilized for each data evaluation and what wind conditions prevailed at the closest observation station(s) that day at 1200 UT, the only observation time available for all sampling dates. The other available observation time, 0000 UT, was available for only a few of the sampling dates, and in none of these cases did the charts indicte conditions significantly different from those that prevailed at 1200 UT. In addition, 1200 UT more closely matches our sampling times.

In our analysis it will be shown, where applicable, that significantly different atmospheric conditions prevailed at the times the two or more NO (NO_x) values under consideration were being obtained, thus suggesting that different air masses were sampled in each case. To determine why the different air masses might have different NO (NO_x) profiles in the same altitude regime lies beyond the scope of this paper. Appropriate references are cited that analyze such behavior in detail.

Referring to the results from Table 3 in order, first, the October 1977 flights at Chico, California, provided values only from one altitude per flight and the flights were conducted 9 days apart. Thus it would not be practical to try to reconstruct a meaningful profile from these results; but in any case, the air mass conditions were significantly different on the two dates; the light and variable winds noted only for October 17 are suggestive of fall turnaround conditions, and the patterns of high and low pressure for the two dates are distinctly different.

The Alaska flights (numbers 13 and 14) produced fairly smooth profiles. The high mixing ratios at 30 km are consistent with most models when viewed in light of the low tropopause that prevailed. All these models show a sharp rise in mixing ratios for the first few kilometers above 30 km, the effective altitude range, vis-a-vis the models, in which this sample was obtained. The principal anomaly in the measured profile is the high value for NO_x at 12 km. Inspection of the charts, however, reveals that although winds in the vicinity of the 15 km sample were light and variable, the 12-km sample was obtained in a strong jet stream, suggestive of a completely different air mass. Of course, for this and for all flights the general features of the local air patterns were observed at the time of the samplings in the process of the tracking of the flight trajectories.

The South Dakota samples were obtained 10 days apart, the largest gap between flights for any single field trip. Also, there was a major difference between the two tropopause heights. A distinct jet stream presence was noted on August 19, 1978, at both sampling altitudes with similar pressure patterns and approximately westerly winds of 20–30 K at 100 mbar and 40–70 K at 200 mbar. It is likely that both the 12- and 15-km samples were obtained in the same large air mass; however, both samples were obtained below the anomalously high tropopause that prevailed, and the 12-km sample could have been affected by the significant aircraft emissions that occur at that altitude; more on this below. For the succeeding flight, a distinctly different pressure and wind pattern existed over North America. On August 29, 1978, a consistent high pressure over the upper Great Lakes region persisted in the 50- to 100-mbar altitude band along with light and variable winds in the region over South Dakota, and with a fairly low tropopause height. The data from the three sampling altitudes are consistent except for the NO_x value at 20 km. This values remains unexplained except for the unlikely possibility that the opposite extremes of the two error bars prevail. The unusually long period between flights, necessitated by adverse

TABLE 4. Wind and Atmospheric Pressure Patterns Relevant to the Air Masses Sampled

Flight No.	Location	Alt., km	Chart		Winds		Relevant Centers of High (H) and Low (L) Pressure
			mbar	Alt., km	Dir.	Speed, knots	
11	Chico	30	10	31.0	W	20	H over S. Calif.
12	Chico	18	50	20.6	SE	10	H over N. Calif. coast
			100	16.2	LV*		L off cent. Calif. coast
13	Eielson	30	10	31.0	E	20	H in E. Siberia
		25	30	23.8	NE	10	H over North Pole
		20	50	20.6	LV		H over Siberia
14	Eielson	15	100	16.2	W	10	No nearby L or H
		12	200	11.8	WSW	45	H in Gulf of Alaska
15	Watertown	15	100	16.2	SW	25	H over SE U.S. and over Calif.
		12	200	11.8	W	55	H over SE U.S. and over Calif.
16	Watertown	30	10	31.0	ENE	10	H over central Canada
		25	30	23.8	NNE	5	H north of Great Lakes
		20	50	20.6	NW	10	H over eastern Great Lakes
17	Panama	18	50	20.6	NE	10	H west of Yucatan Peninsula
		15	100	16.2	W	30	No nearby L or H
18	Panama	30	10	31.0	ESE		H approx. over Yucatan Penin.
		25	30	23.8	LV	5–10	H approx. over Yucatan Penin.
		20	50	20.6	WNW	20	H approx. over Yucatan Penin.
19	Holloman	30	10	31.0	E	30	H near North Pole
		25	30	23.8	ENE	25	H near North Pole
		20	50	20.6	ESE	25	H near North Pole
21	Holloman	18	50	20.6	NW	5	L over central U.S.
		15	100	16.2	WNW	40	L over central U.S.
		12	200	11.8	W	130	L over central U.S.
22	Holloman	30	10	31.0	WNW	20	L over Pacific and H over Atlantic coasts of Mexico
		25	30	23.8	ESE	10	H over lower Calif. coast
		20	50	20.6	LV		L over NM/Col. border
23	Holloman	20	50	20.6	ESE	5	H over central U.S.
		15	100	16.2	WSW	30	L over Hudson Bay
		12	200	11.8	W	45	L over Hudson Bay
24	Holloman	30	10	31.0	E	30	H over S. central Canada
		25	30	23.8	E	30	H over S. central Canada
		20	50	20.6	E	15	H over N. Central U.S.

*LV, light and variable.

surface weather conditions, permitted significantly different air patterns to evolve, as evidenced on the two dates. This situation prevents the construction of a representative profile for this latitude from these five air sample measurements.

As with all the flights, the northern hemisphere charts formed the basis for the evaluation of the March 15 and 20, 1979, results. These charts cut off at about the latitude of Panama. On March 15 an intense low, north of Canada, dominated the pattern for North America at both the 50- and 100-mbar levels. Pressure gradients in the southern Carribbean region were fairly small, however, and at 50 mbar, winds were light NE to NNE at ~10 K. At 100 mbar, they ranged from WSW to WNW at 25–30 K. Thus it would seem that the 18- and 15-km samples were not obtained from the same air mass, thereby providing an explanation for the essentially unchanged value for NO and the modest increase noted for NO_x with decreasing altitude. Five days later on March 20, the 50-mbar charge was not unlike that for the previous date, although the 20-km results are significantly higher than the 18-km values obtained on March 15. The diurnal factor would explain the difference, in part, but the 5-day interval was more than sufficient to suggest a different air mass. More important, the 20-km values are significantly higher than the 25-km results. A low-pressure system is evident on the 50-mbar chart in the sampling region with winds of 10–30 K from the W to NW. At higher altitudes (10 and 30 mbar) the low is not evident and the winds were light and variable. On this basis, it appears that the 25- and 30-km samples were obtained in a different air mass from the 20-km sample. The mixing ratios increase between 25 and 30 km, as expected, albeit at a rapid rate. It will be pointed out below that such high mixing ratios at this latitude are at variance with predictions.

On June 21, 1979, a high near the north pole dominated the pattern at all three altitudes with a consistent wind pattern in the sampling region: E at 30 K at 10 mbar, ENE at 25 K at 30 mbar, and ESE at 25 K at 50 mbar. Not unexpectedly, then, values obtained for NO and NO_x in the 20- to 30-km range showed little variation with altitude.

Data from the 1980 flights (numbers 21 and 22) yielded some of the smoothest profiles obtained in the program. For one thing, weather conditions and logistics at that time permitted the execution of the two sampling flights only 3 days apart, the smallest such interval achieved in the program.

On April 28, 1980, the 50-, 100-, and 200-mbar charts featured a low over the north-central United States and a consistent west to northwest wind, 5 K at 50 mbar, 40 K at 100 mbar, and a distinct jet stream flow of 130 K at 200 mbar. The corresponding NO and NO_x values showed little variation with altitude, consistent with having been obtained from the same air mass as supported by the chart data.

On May 1, 1980, pressure gradients were small over the continental United States with no distinct high or low centers at 10 and 30 mbar and only a weak low in the sampling region evidenced on the 50-mbar chart. Accordingly, winds

were light and variable throughout this altitude range. For example, comparison of the 50-mbar charts for these two 1980 dates indicates that pressure gradients were slight and with similar patterns of high- and low-pressure centers over North America. With these conditions, it is more justifiable to construct a profile from these two flights than from any of the other available options. Although modest increases in both NO and NO_x were noted in descending from 25 to 20 km, these changes are within experimental error, and in part, may reflect also the emergence of the low at 50 mbar. The 30-km mixing ratios are the highest, as expected, although higher than most such values for NO_x. It should be noted, however, that in the development of the various model profiles the tropopause is assumed to exist at some nominal altitude but always higher than 9.6 km for a mid-latitude atmosphere. Therefore this 30 km value represents, effectively, a somewhat higher altitude where all models predict a more rapid change in mixing ratio with altitude. An increase in altitude of only 5 km can very well produce the significant increase in NO_x at 30 km over that noted for 25 km.

Although the "official" tropopause heights are significantly different for the two flight dates, the criteria used to establish this altitude do not always adequately reflect the actual boundary between the troposphere and stratosphere, a boundary that is at times somewhat diffuse and ill defined [*Gallagher et al.*, 1983]. In fact, the example presented in that paper employs the altitude/temperature profiles from these two dates and illustrates the less than ideal profile for May 1, 1980, in comparison to April 28, 1980. Although the official tropopause for May 1 occurred at 9.6 km, the absolute minimum temperature was recorded at about 18 km, thus making the tropopause region quite diffuse and ill defined; nevertheless, the NO_x measurements for that day tend to suppport the official tropopause height.

The profiles for the 1981 flights are fairly smooth, the principal anomaly being the 20-km value for NO_x on May 31. What is most atypical, exclusive of that one measurement, is the "flatness" of the profile, i.e., there is little variation in mixing ratio with altitude for either NO or NO_x. As is shown below, however, similar profiles have been observed elsewhere. On May 31, the 15- and 12-km samples were obtained in a strong jet stream with a low over Hudson Bay evident in both the 100- and 200-mbar charts. On the other hand, the 50-mbar chart (i.e., 20.6 km) exhibited a different pressure pattern with a light ESE wind prevailing, thus suggesting a different air mass for that altitude.

For the flight of June 4, 1981, the mbar charts showed only rather small variations between the 10-, 30-, and 50-mbar levels with a high near the central United States–Canadian border and light easterlies in the region of sampling. The corresponding NO and NO_x measurements responded similarly with an unusally flat response. Conditions that prevailed at 20 km on May 31 and June 4 were not too dissimilar (a consistent high over the central United States), but again, the time factor (4 days) could well have been sufficient to result in different air masses with significantly different NO_x mixing ratios being sampled. Also, some diurnal consideration should be factored into the comparison of the 20-km results.

In summary, we believe that through analysis of the air patterns that existed at the sampling times, we have with few exceptions been able to correlate the general behavior and, especially, the anomalies in the NO and NO_x profiles with the identities of the air masses at adjacent altitudes. In general, a steeper profile than that predicted by the models prevails when two or three succeeding samples were shown to have been obtained in the same air mass. Also, when significant reversals are evident in the profiles, almost invariably they are correlated with distinctly different wind and pressure patterns on the corresponding millibar charts, suggesting a boundary between different air masses between the two sampling altitudes. This supports our conclusion, elaborated upon below, that a significant data base at a given location and time of year is required in order to make meaningful comparison between experimental results and model profiles. Additional considerations include the effects of differences in time (day to day and diurnal) and the location of the tropopause height and, at the lowest altitudes sampled, the risk of aircarft emissions. These additional variables combine to further diminish the reproducibility of suceeding samplings and create a greater difficulty in comparing data with the ideal condition-dependent model profiles for this altitude region.

An additional complication to be addressed concerns the role of peroxyacetyl nitrate (PAN) in the region of the lower altitude samples. PAN has been suggested as an important reservoir for oxides of nitrogen [*Singh and Hanst*, 1981; *Aikin et al.*, 1982, 1983]. PAN, ethane, and other nonmethane hydrocarbons represent significant factors in the transport of combined nitrogen through the atmosphere, yet measurements of these species in this region are scarce. *Aikin et al.* [1982] indicate that PAN is generated throughout the troposphere and lower stratosphere and has a long lifetime with respect to photolysis and rainout, thermal decomposition being the governing factor in the rate of destruction. *Aikin et al.* [1982] also indicate that a fairly significant spread in NO and NO_2 mixing ratios occur below about 15 km, dependent on whether or not PAN concentrations are at the high or low end of the predictions for this altitude region (although the absolute values for NO and NO_2 are somewhat smaller than those reported herein). Also, they indicate that somewhat significant variations in NO_x content can occur, dependent on various potential concentrations of other nonmethane hydrocarbons. PAN is difficult to measure, and measurements in this region are practically nonexistent. Thus effects due to variations in the concentrations of such species content at the relevant altitudes would contribute to the spread in NO and NO_x values at the 12- and 15-km levels.

Another consideration further complicates this point, i.e. the data spread at 12 and 15 km. Exhaust gases from high-altitude aircraft also can have a major effect on the local chemistry. Many of our lower altitude samples were obtained downwind of areas known to experience intense levels of high-altitude aircraft operations. The degree of such effects on a particular sample is impossible to determine. A coordinated, controlled experiment would be required to delineate such influences. As concerns our current data, it is only possible to speculate that such influences did exist. The total of such emissions is not insignificant. Recently, *Wuebbles et al.* [1983] summarized estimates of past and future aircraft emissions of NO_x (as NO_2) to altitudes of 20 km. For example, at 12 km, northern hemisphere values are assumed to increase linearly from about 50 metric tons per year in 1975 to over 300 metric tons per year by 1990. In addition, NO and NO_2 are sensitive to trace concentrations of hydrocarbons [*Aikin et al.*, 1982] as indicated above, and hydrocarbon concentrations in the vicinity of and below the tropopause can reflect aircraft emissions.

Expanding on another factor mentioned above, the duration of sampling, i.e., the time from initiation of the first sampling to the termination of the third sampling at the final

altitude, can extend over a period of as much as 5 hours, during which normal diurnal as well as other atmospheric variations can occur. Furthermore, the three samples gathered on most AFGL balloon flights were obtained over a significant horizontal range that for some flights exceeded 300 km. The point, then, is that although this time frame is quite acceptable for the generation of a meaningful measured profile for stable species [e.g., *Gallagher et al.*, 1983], it is probably not so for reactive species.

Keeping all these factors in mind, the problem becomes how best to compare measured results with model predictions and with experimental results reported elsewhere. From the preceding analysis, it is concluded that it is more appropriate to compare only averages of experimental results with model profiles, since the latter are developed for invariant nominal conditions. This situation can be approximated experimentally only by the creation of a sufficient data base so as to largely average out many of the perturbing influences. Consistent with this conclusion, the emphasis below centers on comparison of other results and model profiles with averages of AFGL data from one location obtained at approximately the same time of year and limited to a period of only a few years.

With the above in mind, the AFGL results for NO from our largest data base (i.e., the results obtained from the Holloman Air Force Base (HAFB) flights conducted between 1979 and 1981) are compared with representative values obtained elsewhere as shown in Figure 3. The comparison data were obtained from a variety of experimental approaches including balloon- and rocket-borne chemiluminescence analyzers and from various spectral observations. Of course, latitudinal, seasonal, and diurnal differences occur among the various observations obtained elsewhere, but we have attempted to compare data obtained only under conditions not dramatically different from these under which our data were collected. In what follows, we point out the more salient features relevant to these observations and cite individual papers for particulars.

Roy et al. [1980] employed a balloon-borne chemiluminescence detector to obtain vertical profiles of NO in the stratosphere. Two flights were conducted from Australia (34 S) and one flight from Texas (32 N). Resultant profiles from both locations are in good agreement. The authors suggest the distribution of nitric oxide at low latitudes may be symmetric about the equator. An average profile constructed from their results is included in Figure 3. No Texas data are available below about 15 km. Data were obtained primarily on ascent, and the more limited data obtained on parachute descent are considered by the authors to be less accurate and thus were not included in preparing the average profile displayed in Figure 3.

Ridley and Hastie [1981] obtained values for NO at 51°N using a balloon-borne chemiluminescence instrument. Profiles from two of those flights are contained in Figure 3. Profile A was obtained on August 19, 1976, and profile B on August 28, 1976. Although the authors obtained closely spaced discrete data points, the results have been plotted in Figure 3 as continuous curves for convenience. A leak occurred in the balloon for the earlier (A) flight, and the authors expressed a lower degree of confidence in that data.

Blatherwick et al. [1980] obtained infrared solar spectra at ~0.02 cm^{-1} resolutions at sunset from a balloon platform. Six scans, each for a different solar zenith angle, were all obtained at 33 km. From the resulting spectra and a simple photochemical model, they derived simultaneous values of

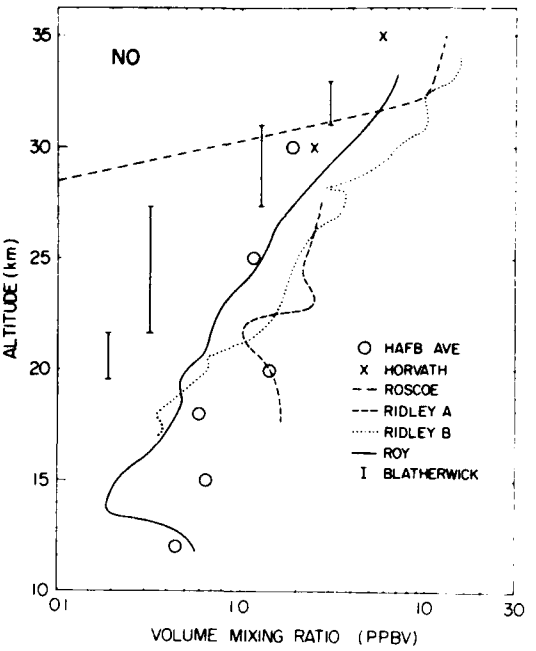

Fig. 3. Average of results for NO from Holloman Air Force Base, New Mexico, 1979–1981, compared with representative results from other experiments (for details, see text).

mixing ratio profiles of NO and NO_2. Values for NO from five of the six layers are shown in Figure 3. The lowest layer is just off scale at 0.098 ppbv.

A rocket-borne, parachute-deployed chemiluminescence instrument provided *Horvath et al.* [1983] with nitric oxide profiles covering the range 30–50 km. Their average mid-latitude data are included in Figure 3 for altitudes of 30 and 35 km. They point out that the summertime spread in data at 30 km (as well as at 40 km) is very large.

The Oxford balloon-borne pressure modulator radiometer was used to provide altitude profiles of NO and NO_2 simultaneously, from mid-morning till sunset [*Roscoe et al.*, 1981]. Mixing ratio profiles averaged for the entire daytime flight of September 20, 1978, at Palestine, Texas (32°N), are presented for the 20- to over 50-km altitude range, and the portion of the NO profile below 35 km is reproduced in Figure 3.

Figure 4 contains the NO + NO_2 values corresponding to the NO data presented in Figure 3 for those investigations that provided simultaneous determinations of NO and NO_2. Unfortunately, no such profiles exist which correspond to the three NO profiles that most closely match the AFGL data in Figure 3. However, the values of NO for all three of those curves in the 17- to 20-km range are alone, close to, or already higher than the NO + NO_2 values reported by Blatherwick, and a comparison with Roscoe's NO + NO_2 results exhibits an even greater difference in the same sense.

Mount et al. [1984] reported daytime measurements of NO_2 for the 20- to 40-km region over nearly the complete latitudinal range, based on NO_2 absorption in sunlight scattered from the atmosphere and as observed by a visible light spectrometer on board the Solar Mesospheric Explorer (SME) spacecraft. They noted good agreement with several other measurements, including some cited here.

Figure 5 contains a plot of the NO_2/NO ratio as a function of altitude for the average of all our mid-latitude (33–45°N) data. The figure also includes the envelope for the calculated ratio obtained by *Ridley and Hastie* [1981] assuming a photo-

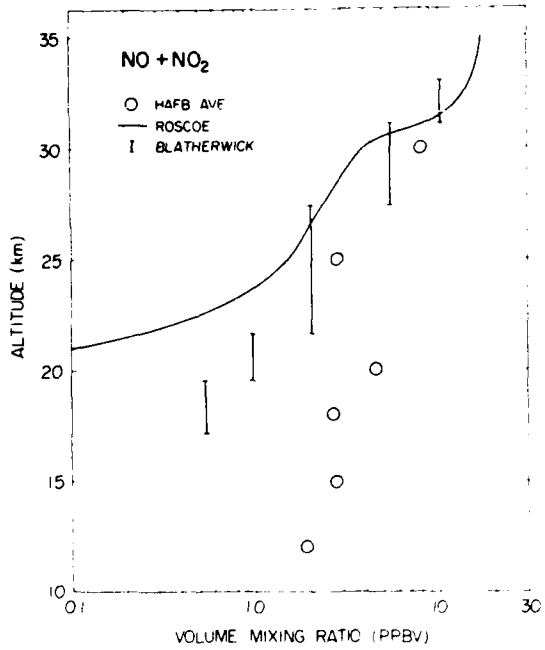

Fig. 4. Average of results for $NO + NO_2$ from Holloman Air Force Base, New Mexico, 1979–1981, compared with results from others cited in Figure 3 who provided data for both NO and NO_2.

chemical steady state situation. The envelope allows for a $\pm 20\%$ uncertainty in the photodissociation coefficient of NO_2. These authors also combined their NO results with NO_2 data obtained from a separate experiment to produce their measured NO_2/NO values shown in Figure 5. Since they used two separate values for NO_2 at each altitude, the ranges of their determinations are illustrated using horizontal bars. The NO and NO_2 data of *Roscoe et al.* [1981] yield the curve in Figure 5 which greatly exceeds the scale limit below 30 km. The Blatherwick data from Figures 3 and 4 produce the vertical bars. The AFGL results are seen to be close to and generally bracketed by all the comparison results. All of the measured results exceed model predictions below about 25 km. *Ridley and Hastie* [1981] point out that the calculated range does not include the uncertainty in the rate coefficients, k_{NO/O_3}, or in the measurements of certain parameters such as O_3 and temperature. Other factors that affect comparison between our results and atmospheric models have been discussed already. The $NO + NO_2$ values implied by the Ridley and Hastie data from Figure 5 are more consistent with the AFGL data than with the model profiles at the lower altitudes in Figure 4.

The AFGL balloon flights were conducted from various launch sites in order to assess latitudinal dependence for the species studied. Comparison of the averages of all mid-latitude data (primarily obtained in the late spring and summer) with the limited results from Alaska and Panama (spring) failed to indicate any clear trend common to all altitudes, but did suggest a mid-latitude diminution for NO throughout the altitude range and increasing NO_2 with increasing latitude only for the higher altitudes. The NO results contradict the 18- and 21-km spring observations and two-dimensional model predictions reported by *Lowenstein et al.* [1978]. Of course, as indicated above, more than one set of data is required at a given location in order to be able to construct a representative profile for that location for reactive species, and results from only a single series are available for Alaska and Panama. The AFGL flight demonstrated latitudinal dependence for several stable trace species [*Gallagher et al.*, 1983] for which diurnal and other natural variables are less significant and for which the measurement uncertainty is also less.

HNO_3 plays a significant role in both the stratospheric odd nitrogen and oxygen budgets, but HNO_3 measurements were not included in our program. *Coffey et al.* [1981] have summarized results from various measurements of stratospheric HNO_3 (as well as NO_x). The range of HNO_3 values within the 12- to 20-km altitude band varies by more than an order of magnitude. Thus the total odd nitrogen content at these altitudes can be the same if a high NO_x content is coincident with a low HNO_3 content and vice versa.

The averages of our NO and $NO + NO_2$ results from the Holloman Air Force Base flights, 1979–1981, have been evaluated in terms of four representative models (three two-dimensional models and a single one-dimensional model). Figure 6 presents the AFGL data for NO and $NO + NO_2$ from Figures 3 and 4 along with profiles from three of the models. *Sze et al.* [1982] developed a one-dimensional, steady state model with photochemical equilibrium applied to NO and NO_2. It predicts a greater abundance of NO than was predicted previously by the model, the change being a consequence of downward revisions in the predicted OH abundance below 30 km.

A major stratospheric sink for NO_2 is the reaction with OH. The reaction rates for

$$OH + HNO_3 \rightarrow H_2O + NO_3$$

and

$$OH + HNO_4 \rightarrow H_2O + \text{products}$$

have been revised upward [see, e.g., *Sze et al.*, 1980]. The dominant sinks for HO_x below 30 km are therefore now affected by these reactions. The reaction:

$$OH + HO_2 \rightarrow H_2O + O_2$$

was thought to be the major sink for stratospheric HO_x and the lack of data below 30 km prevented confirmation of the

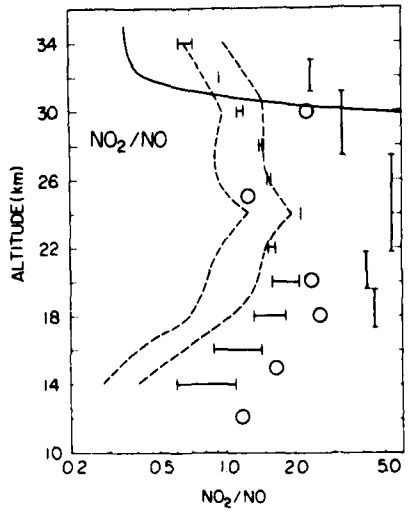

Fig. 5. NO_2/NO ratios for the averages of our mid-latitude results (circles) are compared with results reported by *Ridley and Hastie* [1981] (horizontal bars) and as determined from results reported by *Blatherwick et al.* [1980] (vertical bars). The solid curve is based on results reported by *Roscoe et al.* [1981]. The envelope of the ratios predicted by a photochemical model [*Ridley and Hastie*, 1981] (dashed lines) is included for comparison.

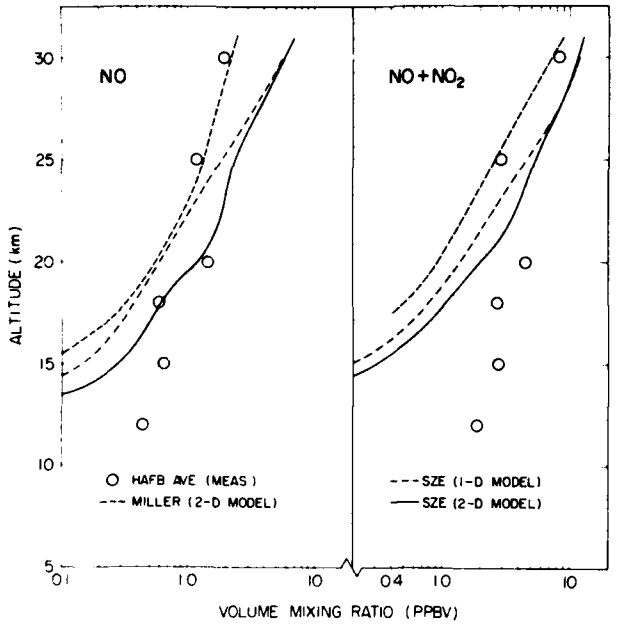

Fig. 6. NO and NO + NO_2 averages from Holloman Air Force Base (HAFB) flights, 1979–1981, are compared with profiles from one- and two-dimensional models.

model in this region. More recent models assume that the OH abundance below 30 km was overestimated, and new laboratory measurements support this hypothesis. As a result of these studies, the predicted OH concentration below 30 km is about a factor of 2 to 3 smaller than predicted by earlier models. With lower values for OH below 30 km, and with OH being a major sink for NO_2 via the reaction, OH + NO_2, significantly higher NO and NO_x concentrations in the stratosphere below 30 km are expected, a conclusion corroborated by our results. In any case, a high level of agreement cannot be expected between any single measurement and one-dimensional model predictions due to the significant horizontal transport.

Sze et al. [1982] also developed a two-dimensional model to simulate the zonal-mean behavior of atmospheric trace gases. A slight update of the published model is included in Figure 6. Although a two-dimensional model has the advantage of simulating atmospheric latitudinal gradients and seasonal behavior, current models are not completely developed from first principles. Transport is partly parameterized by eddy diffusion coefficients derived from other observations. Since our observations at 12 and 15 km are larger than most such observations reported elsewhere, it may not be surprising that the models do not closely agree with our observations at these altitudes.

Miller et al. [1981] developed a two-dimensional model of the stratosphere with 30 active species. Most species are transported and calculated separately, with the transport scheme containing both diffusive and advective terms. The authors point out significant discrepancies between experiment and theory for the oxides of nitrogen.

Garcia and Solomon [1983] developed a two-dimensional, time-dependent model to study the zonally averaged structure of the middle atmosphere, allowing interaction among dynamics, radiation, and photochemistry. They point out, as have others, that one-dimensional models do not include the effect of meridional transport. Their model profile for NO at 32°N exhibits an annual range of roughly 1.5–2 ppbv at 30 km but drops below 1 ppbv in the 25- to 28-km range. Thus although the model provides a fairly close match to our measured averages at 25 and 30 km (see Figure 6), it provides a poorer match to the lower altitude measurements than do the models illustrated. The high-latitude (75°N) NO profile exhibits considerable seasonal variability at the higher altitudes (40–100 km) but remains constant at about 5 ppbv at 30 km and decreases to about 1.3 ppbv at 20 km. This behavior is not too different than the single profile obtained by AFGL at 64°N. The greater NO densities in the lower stratosphere in summer at the higher latitudes are attributed to downward advection from the upper stratosphere of air rich in NO_x. At low latitudes, NO densities are thought to be low, since rising motion there, as postulated, advects air of low NO_x content from the tropical tropopause. Such predictions, however, are at variance with our limited data from 9°N. The subject report does not include the corresponding NO_2 profiles, although it is pointed out that large values occur at high latitudes in the lower stratosphere primarily due to the advection of NO_x from the upper stratosphere, a variation consistent with our limited measurements at 64°N.

4. CONCLUSIONS

Measurements of the mixing ratios of the stratospheric trace gas species NO and NO_x have been obtained using a direct sampling method, one of the few such methods that provides NO and NO_x values simultaneously. Coverage of several altitudes and latitudes contributes to the data base that permits comparison with, and possibly updating of, stratospheric models relative to transport and chemistry. Since the measured values are generally greater than those predicted by most models for the lower regions of the stratosphere, they suggest that for a given NO_2 injection, the percentage change in stratospheric NO_x from such a perturbation should be even less significant than would be the case if a lower background concentration prevailed.

Although most other mixing ratios reported in the literature are lower than those reported here, particularly below 20 km, other results similar to ours have also been cited. This supports our conclusion that significant variability in stratospheric NO and NO_2 mixing ratios exists, with the ranges well exceeding anything attributable merely to experimental error. Much of the variability in our data has been successfully correlated with variations in atmospheric motions determined from the relevant pressure and wind patterns. This strongly suggests that only averages from a series of experimental profiles obtained under similar seasonal and diurnal conditions should be used for inputs to, and comparison with, model profiles for reactive species such as the oxides of nitrogen. The effects of transport on the abundances of the oxides of nitrogen have been discussed at length by others as referenced above. Also our results show that the more nearly the same air patterns persist over a wide altitude band, the steeper are the mixing ratio profiles for that flight. This is suggestive of significant uniformity in NO_x mixing ratios within a given air mass, somewhat regardless of altitude, at least for the altitude range reported herein. Additional complications due to the role of PAN in the vicinity of the tropopause, plus variations in tropopause height and, to a lesser extent, the diurnal, seasonal, and horizontal trajectory, all combine to influence the measured profiles and comparisons with model profiles. Add to this the local variable of aircraft injections at the lowest altitudes, and a further variance in data is inevitable. With limited observations, latitudinal variations were not clear cut

and differed from other reported observations and model predictions.

Acknowledgments. The late Rocco S. Narcisi initiated this study. The authors with to thank Hans Laping and Alan Bailey for electronics design, John Borghetti and Anthony Coriaty for their generous assistance, both in the laboratory and field programs, and John Ground, Richard Ganion, Ronald Lavigne, and the many others within the AFGL Aerospace Instrumentation Division and Balloon Launch Facility whose invaluable assistance is very much appreciated. We also thank Patricia Bench for running the computer programs and Pauline Beardsley for her patience in typing the manuscript.

REFERENCES

Addison, W. E., and R. M. Barrer, Sorption and reactivity of nitrous oxide with nitric oxide in crystalline and amorphous siliceous sorbents, *J. Chem. Soc. London*, 757–769, 1955.

Aikin, A. C., J. R. Herman, E. J. Maier, and C. J. McQuillan, Atmospheric chemistry of ethane and ethylene, *J. Geophys. Res.*, *87*, 3105–3118, 1982.

Aikin, A. C., J. R. Herman, E. J. R. Maier, and C. J. McQuillan, Influence of peroxyacetyl nitrate (PAN) on odd nitrogen in the troposphere and lower stratospehre, *Planet. Space Sci.*, *31*, 1075–1082, 1983.

Blatherwick, R. D., A. Goldman, D. G. Murcray, F. J. Murcray, G. R. Cook, and J. W. Van Allen, Simultaneous mixing ratio profiles of stratospheric NO and NO_2 as derived from balloon-borne infrared solar spectra, *Geophys. Res. Lett.*, *7*, 471–473, 1980.

Calo, J. M., Composition alteration of stratospheric air due to sampling through a flow tube, *Tech. Rep. AFGL-TR-84-0045*, Air Force Geophys. Lab., Hanscom Air Force Base, Mass., 1984.

Calo, J. M., R. J. Fezza, and E. J. Dineen, Gas-surface interactions in cryogenic whole air sampling, *Tech. Rep. AFGL-TR-81-0162*, Air Force Geophys. Lab., Hanscom Air Force Base, Mass., 1981.

Coffey, M. T., W. G. Mankin, and A. Goldman, Simultaneous spectroscopic determination of the latitudinal, seasonal, and diurnal variability of stratospheric N_2O, NO, NO_2, and HNO_3, *J. Geophys. Res.*, *86*, 7331–7341, 1981.

Fabian, P., J. A. Pyle, and R. J. Wells, Diurnal variations of minor constituents in the stratosphere modeled as a function of latitude and season, *J. Geophys. Res.*, *87*, 4981–5000, 1982.

Federal Aviation Administration, Upper atmospheres programs bulletin, Report on HAPP Scientific Advisory Meeting, *81-1*, p. 1, Washington, D C., 1981.

Fezza, R. J., and J. M. Calo, Atmospheric gases on cold surfaces—Condensation, thermal desorption and chemical reactions, in *Heterogeneous Atmospheric Chemistry, Geophys. Monogr. 27*, edited by D. Schryer, AGU, Washington, D. C., 1982.

Gallagher, C. C., and C. A. Forsberg, Observations of major stratospheric chlorine species, *Tech. Rep. AFGL-TR-83-0284 (AD A138646)*, Air Force Geophys. Lab., Hanscom Air Force Base, Mass., 1983.

Gallagher, C. C., C. A. Forsberg, R. V. Pieri, and G. A. Faucher, Stratospheric trace gas composition studies utilizing in situ cryogenic, whole air sampling methods, *Tech. Rep. AFGL-TR-81-0071*, Air Force Geophys. Lab., Hanscom Air Force Base, Mass., 1981.

Gallagher, C. C., C. A. Forsberg, and R. V. Pieri, Stratospheric N_2O, CF_2Cl_2, and $CFCl_3$ composition studies utilizing in situ cryogenic, whole air sampling methods, *J. Geophys. Res.*, *88*, 3798–3808, 1983.

Garcia, R. R., and S. Solomon, A numerical model of the zonally averaged dynamical and chemical structure of the middle atmosphere, *J. Geophys. Res.*, *88*, 1379–1400, 1983.

Horvath, J. J., J. E. Frederick, N. Orsini, and A. R. Douglass, Nitric oxide in the upper stratosphere: Measurements and geophysical interpretation, *J. Geophys. Res.*, *88*, 10,809–10,817, 1983.

Johnston, H. S., Reduction of stratospheric ozones by nitrogen oxide catalysts from supersonic transport exhaust, *Science*, *173*, 517–522 1971.

Kramer, M. A., R. J. Kee, and H. Rabitz, CHEMSEN: A computer code for sensitivity analysis of elementary chemical reaction models, *Tech. Rep. SAND 82-8230*, Sandia Nat. Lab., Livermore, Calif., 1982.

Lowenstein, M., W. L. Starr, and D. G. Murcray, Stratospheric NO and HNO_3 observations in the northern hemisphere for three seasons, *Geophys. Res. Lett.*, *5*, 531–534, 1978.

Lucas, D., and G. C. Pimentel, Reaction between nitric oxide and ozone in solid nitrogen, *J. Phys. Chem.*, *83*, 2311–2316, 1979.

Miller, C., D. L. Filkin, A. J. Owens, J. M. Steed, and J. P. Jesson, A two-dimensional model of stratospheric chemistry and transport, *J. Geophys. Res.*, *86*, 12,039–12,065, 1981.

Molina, M. J., and F. S. Rowland, Stratospheric sink for chlorofluoromethanes: Chlorine-atom catalyzed destruction of ozone, *Nature*, *249*, 810–815, 1974.

Mount, G. H., D. W. Rusch, J. F. Noxon, J. M. Zawodny, and C. A. Barth, Measurements of stratospheric NO_2 from the solar mesosphere explorer satellite 1, An overview of the results, *J. Geophys. Res.*, *89*, 1327–1340, 1984.

National Aeronautics and Space Administration, Chemical kinetics and photochemical data for use in stratospheric modeling, *Eval. 5*, Jet Propulsion Lab., Pasadena, Calif., 1982.

National Research Council, *Causes and Effects of Changes in Stratospheric Ozone: Update 1983*, National Academy Press, Washington, D. C., 1983.

Noxon, J. F., W. R. Henderson, and R. B. Norton, Stratospheric NO_2, 3, The effects of large-scale horizontal transport, *J. Geophys. Res.*, *88*, 5240–5248, 1983.

Oliver, R. C., E. Bauer, H. Hidalgo, K. A. Gardner, and W. Wasylkiwskyj, Aircraft emissions, potential effects on ozone and climate, *HAPP Tech. Rep. FAA-EQ-77-3*, Dept. of Transport., Washington, D. C., 1977.

Ridley, B. A., and D. R. Hastie, Stratospheric odd-nitrogen: NO measurements at 51°N in summer, *J. Geophys. Res.*, *86*, 3162–3166, 1981.

Roscoe, H. K., J. R. Drummond, and R. F. Jarnot, Infrared measurements of stratospheric composition, III, The daytime changes of NO and NO_2, *Proc. R. Soc. London, A375*, 507–528, 1981.

Roy, C. R., I. E. Galbally, and B. A. Ridley, Measurements of nitric oxide in the stratosphere of the southern hemisphere, *J. R. Meteorol. Soc.*, *106*, 887–894, 1980.

Schmeltekopf, A. L., P. D. Goldan, W. J. Harrop, T. L. Thompson, D. L. Albritton, M. McFarland, A. E. Sapp, and W. R. Henderson, Balloon-borne stratospheric grab-sampling system, *Rev. Sci. Instrum.*, *47*, 1479–1485, 1976.

Singh, H. B., and P. L. Hanst, Peroxyacetyl nitrate (PAN) in the unpolluted atmosphere: An important reservoir for nitrogen oxides, *Geophys. Res. Lett.*, *8*, 941–944, 1981.

Smith, A. L., W. E. Keller, and G. L. Johnston, The infrared and Raman spectra of condensed nitric oxide, *J. Chem. Phys.*, *19*, 189–192, 1951.

Smith, G. R., and W. E. Guillory, The kinetics of the thermal oxidation of NO in solid oxygen between 13 and 29 K: Direct observation of the reaction of $(NO)_2$ and oxygen, *Int. J. Chem. Kinet.*, *9*, 953 968, 1977.

Sze, N. D., N. K. W. Ko, R. Specht, and M. Livshits, Modelling of chemical processes in the troposphere and stratosphere, *Tech. Rep. AFGL-TR-80-0251*, Air Force Geophys. Lab., Hanscom Air Force Base, Mass., 1980.

Sze, N. D., M. K. W. Ko, M. Livshits, W. C. Wang, and P. B. Ryan, A research program for atmospheric chemistry, radiation and dynamics, *Tech. Rep. AFGL-TR-82-0207*, Air Force Geophys. Lab., Hanscom Air Force Base, Mass., 1982.

World Meteorological Organization, The stratosphere 1981: Theory and measurements, *Global Ozone Res. and Monitoring Proj. Rep. 11*, Geneva, 1982.

Wuebbles, D. J., F. M. Luther, and J. E. Penner, Effect of coupled anthropogenic perturbations on stratospheric ozone, *J. Geophys. Res.*, *88*, 1444–1456, 1983.

J. M. Calo, G. A. Faucher, C. A. Forsberg, C. C. Gallagher, and R. Pieri, Air Force Geophysics Laboratory, Hanscom Air Force Base, 01731-5000.

(Received May 18, 1984;
revised January 29, 1985;
accepted February 1, 1985.)

Unclassified
SECURITY CLASSIFICATION OF THIS PAGE

REPORT DOCUMENTATION PAGE

1a. REPORT SECURITY CLASSIFICATION: Unclassified	1b. RESTRICTIVE MARKINGS
2a. SECURITY CLASSIFICATION AUTHORITY	3. DISTRIBUTION/AVAILABILITY OF REPORT: Approved for public release; Distribution unlimited.
2b. DECLASSIFICATION/DOWNGRADING SCHEDULE	
4. PERFORMING ORGANIZATION REPORT NUMBER(S): AFGL-TR-85-0231	5. MONITORING ORGANIZATION REPORT NUMBER(S)
6a. NAME OF PERFORMING ORGANIZATION: Air Force Geophysics Laboratory; 6b. OFFICE SYMBOL (If applicable): LID	7a. NAME OF MONITORING ORGANIZATION
6c. ADDRESS (City, State and ZIP Code): Hanscom AFB, Massachusetts 01731	7b. ADDRESS (City, State and ZIP Code)
8a. NAME OF FUNDING/SPONSORING ORGANIZATION; 8b. OFFICE SYMBOL (If applicable)	9. PROCUREMENT INSTRUMENT IDENTIFICATION NUMBER
8c. ADDRESS (City, State and ZIP Code)	10. SOURCE OF FUNDING NOS.

PROGRAM ELEMENT NO.	PROJECT NO.	TASK NO.	WORK UNIT NO.
61102F	2310	G3	16

11. TITLE (Include Security Classification) Nitric Oxide and Nitrogen Dioxide Content of Whole Air Samples Obtained at Altitudes From 12 to 30 km

12. PERSONAL AUTHOR(S) Charles C. Gallagher, Charles A. Forsberg, Robert V. Pieri, Gerald A. Faucher, Joseph M. Calo

13a. TYPE OF REPORT	13b. TIME COVERED	14. DATE OF REPORT (Yr., Mo., Day)	15. PAGE COUNT
REPRINT	FROM _____ TO _____	1985 October 7	14

16. SUPPLEMENTARY NOTATION
Reprinted from J of Geophysical Research, Vol 90, #D5, 20 August 1985

17. COSATI CODES			18. SUBJECT TERMS (Continue on reverse if necessary and identify by block number)
FIELD	GROUP	SUB. GR.	Nitric oxide Nitrogen dioxide Stratosphere

19. ABSTRACT (Continue on reverse if necessary and identify by block number)

Whole air samples were obtained in the stratosphere using a liquid helium-cooled cryosampler mounted on a balloon platform. Approximately 1 g mol of sample was obtained at each of three altitudes per balloon flight and was maintained at 4 K until desorption just prior to analysis. Samples were obtained at six altitudes ranging from 12 to 30 km and at five latitudes from 9° to 64°N. Nitric oxide and the sum of nitric oxide and nitrogen dioxide content of the samples were determined using two chemiluminescence analyzers. Results from flights conducted between 1977 and 1981 are correlated with atmospheric motions and other significant variables and evaluated in terms of both one- and two-dimensional models of the stratosphere.

20. DISTRIBUTION/AVAILABILITY OF ABSTRACT	21. ABSTRACT SECURITY CLASSIFICATION
UNCLASSIFIED/UNLIMITED ☐ SAME AS RPT. ☒ DTIC USERS ☐	Unclassified

22a. NAME OF RESPONSIBLE INDIVIDUAL	22b. TELEPHONE NUMBER (Include Area Code)	22c. OFFICE SYMBOL

DD FORM 1473, 83 APR EDITION OF 1 JAN 73 IS OBSOLETE.

Unclassified
SECURITY CLASSIFICATION OF THIS PAGE

END

FILMED

12-85

DTIC